Early-life heterologous rhinovirus infections induce an exaggerated asthma-like phenotype

Charu Rajput, PhD,[a]* Mingyuan Han, PhD,[a]* Tomoko Ishikawa, MS,[a] Jing Lei, BS,[a] Seyedehzarifeh Jazaeri, MD,[a] J. Kelley Bentley, PhD,[a] and Marc B. Hershenson, MD[a,b] *Ann Arbor, Mich*

GRAPHICAL ABSTRACT

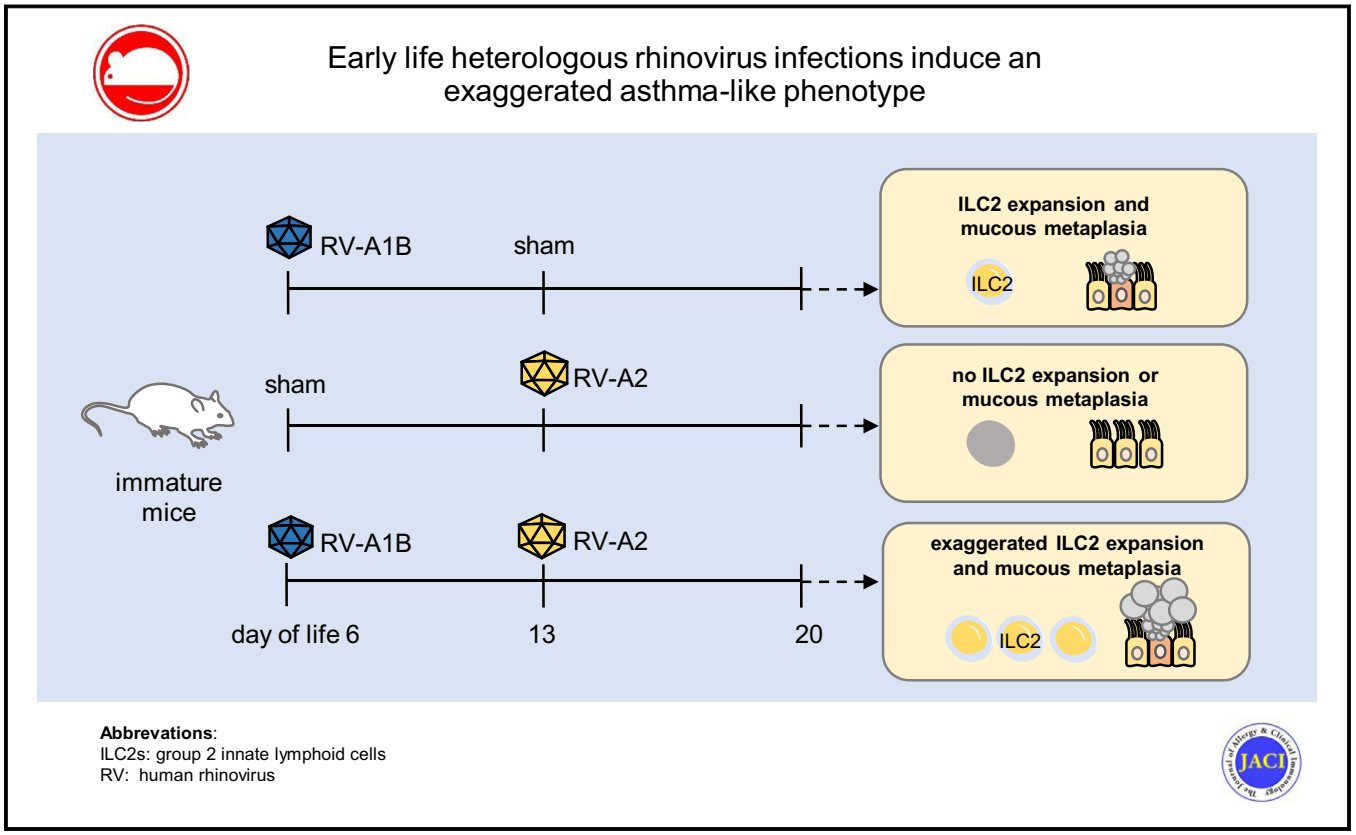

Background: Early-life wheezing-associated respiratory tract infection by rhinovirus (RV) is a risk factor for asthma development. Infants are infected with many different RV strains per year.

Objective: We previously showed that RV infection of 6-day-old BALB/c mice induces a mucous metaplasia phenotype that is dependent on type 2 innate lymphoid cells (ILC2s). We hypothesized that early-life RV infection alters the response to subsequent heterologous infection, inducing an exaggerated asthma-like phenotype.

Methods: Wild-type BALB/c mice and *Rora*$^{fl/fl}$*Il7r*^{cre} mice lacking ILC2s were treated as follows: (1) sham on day 6 of life plus sham on day 13 of life, (2) RV-A1B on day 6 plus sham on day 13, (3) sham on day 6 plus RV-A2 on day 13, and (4) RV-A1B on day 6 plus RV-A2 on day 13.

Results: Mice infected with RV-A1B at day 6 and sham at day 13 showed an increased number of bronchoalveolar lavage eosinophils and increased expression of IL-13 mRNA but not expression of IFN-γ mRNA (which is indicative of a type 2 immune response), whereas mice infected with sham on day 6 and RV-A2 on day 13 of life demonstrated increased IFN-γ expression (which is a mature antiviral response). In contrast, mice infected with RV-A1B on day 6 before RV-A2 infection on day 13 showed increased expression of IL-13, IL-5, Gob5,

From [a]the Department of Pediatrics and [b]the Department of Molecular and Integrative Physiology, University of Michigan Medical School, Ann Arbor.

*These authors contributed equally to this work.

This work was supported by the National Institutes of Health (grant R01 AI120526 [to M.B.H.]).

Disclosure of potential conflict of interest: The authors declare that they have no relevant conflicts of interest.

Received for publication September 3, 2019; revised March 11, 2020; accepted for publication March 26, 2020.

Available online April 25, 2020.

Corresponding author: Marc B. Hershenson, MD, Medical Sciences Research Building II, 1150 W Medical Center Drive, Ann Arbor, MI. E-mail: mhershen@umich.edu.

The CrossMark symbol notifies online readers when updates have been made to the article such as errata or minor corrections

0091-6749/$36.00

https://doi.org/10.1016/j.jaci.2020.03.039

Muc5b, and Muc5ac mRNA; increased numbers of eosinophils and IL-13–producing ILC2s; and exaggerated mucus metaplasia and airway hyperresponsiveness. Compared with *Rora*$^{fl/fl}$ mice, *Rora*$^{fl/fl}$*Il7r*^{cre} mice showed complete suppression of bronchoalveolar lavage eosinophils and mucous metaplasia.
Conclusion: Early-life RV infection alters the response to subsequent heterologous infection, inducing an intensified asthma-like phenotype that is dependent on ILC2s. (J Allergy Clin Immunol 2020;146:571-82.)

Key words: *Asthma, childhood, early-life, IL-13, rhinovirus, RV-A1B, RV-A2, trained immunity, type 2 innate lymphoid cell, ILC2*

Abbreviations used
BAL: Bronchoalveolar lavage
DAPI: 4′,6-Diamidino-2-phenylindole
ILC2: Type 2 innate lymphoid cell
PAS: Periodic acid–Schiff
RSV: Respiratory syncytial virus
RV: Human rhinovirus
SRY: Sex-determining region Y
vRNA: Viral RNA

Early-life wheezing-associated respiratory tract infections by human rhinovirus (RV) and respiratory syncytial virus (RSV) are considered risk factors for asthma development.[1-7] Children are infected with many different RV strains, with infants having 6 to 10 distinct RV infections per year.[8] RV infections do not induce specific immunity to reinfection by heterologous serotypes, even if viruses are from the same species (eg, RV-A1A and RV-A2).[9,10] RVs are divided into 3 species (A, B, and C), which comprise more than 160 antigenically distinct strains. Recurrent RV infections could result in greater degrees of airway inflammation and the potential for airway remodeling and loss of lung function over time.[5,11,12]

In the Tucson Children's Respiratory Study, which is a prospective birth cohort study, lower respiratory tract illness with RSV before 3 years of age was an independent risk factor for the development of wheezing up to age 11 years but not at 13 years.[6] Infants with severe RSV[7] and RV[1] infections requiring hospitalization are more likely to have asthma at ages 13 and 7 years, respectively. In the University of Wisconsin Childhood Origins of Asthma birth cohort of infants at increased risk of asthma, wheezing with RV in the first 3 years of life was strongly associated with asthma at 6 and 13 years of age.[2,4,13] In contrast to RV, RSV had a lessened impact with time. RV and allergic sensitization had additive effects on asthma risk. In the Western Australian Pregnancy Cohort Study, wheezing lower respiratory illness in the first year of life increased the risk for asthma at the age of 6 years in both children without atopic disease and children with atopic disease.[14] In the Perth Childhood Asthma Study of children at high atopic risk, asthma at 5 years of age was associated with early-life wheezy and/or febrile lower respiratory tract infection.[15] However, the associations were restricted to children who displayed allergen sensitization. In The Netherlands Generation R study, those children with bronchitis, bronchiolitis, and pneumonia before 3 years of age were more likely to have asthma and lower lung function at 10 years of age.[12] Allergic sensitization did not factor into the associations seen. Together, these data suggest that early-life respiratory viral infection, in particular with RV, may contribute to the development of asthma, in some cases in the absence of allergen sensitization.

Infection of immature mice with RSV predisposes to the development of IL-13–dependent airway eosinophilia and airways hyperresponsiveness after homologous reinfection 5 weeks later, whereas infection at weaning protects against reinfection.[16,17] These data are consistent with the notion that early-life RSV infection polarizes the adaptive immune response in such a way that homologous reinfection stimulates type 2 immune responses. However, the effect of early-life heterologous RV infections, which are much more common, has not been studied. We have previously shown that RV infection of 6-day-old BALB/c mice, but not mature mice, induces an asthma-like phenotype that is associated with type 2 innate lymphoid cell (ILC2) expansion and dependent on IL-13, IL-25, and IL-33.[18,19] We found that ILC2s persisted longer than 3 weeks after infection.[18] These data are consistent with the notion that following early-life RV-induced expansion, ILC2s could form a stable population of innate immune cells capable of responding to subsequent heterologous infections, a form of trained immunity.[20]

To examine the effects of heterologous RV infections on airway responses, we infected immature mice with different RV strains (RV-A1B and RV-A2) on days 6 and 13 of life, measuring airway responses 1 week after the second infection. We hypothesized that RV-A1B infection on day 6 would alter the immune response to heterologous infection with RV-A2 on day 13 of life, inducing an exaggerated asthma-like phenotype. We found that early-life heterologous infection with RV-A1B and RV-A2 induced intensified type 2 eosinophilic inflammation and mucous metaplasia that was dependent, at least in part, on ILC2s.

METHODS

Animals

All animal use was approved by the Institutional Animal Care and Use Committee and followed guidelines set forth in the Principles of Laboratory Animal Care from the National Society for Medical Research. BALB/c mice were purchased from Jackson Laboratory (Bar Harbor, Maine) and bred in-house in pathogen-free facility within the Unit for Laboratory Animal Medicine at the University of Michigan. The *Rora*$^{fl/fl}$, *Rora*$^{fl/fl}$*IL7R*^{cre}, and *IL7R*^{cre} mice were a gift from Dr Andrew Mckenzie (MRC Laboratory of Molecular Biology, Cambridge, United Kingdom). Six day-old mice were used for the experiments.

Generation of RV-A1B and RV-A2

RV-A1B and RV-A2 (ATCC, Manassas, Va), which are minor group viruses that infect mouse cells,[21] were partially purified from infected HeLa cell lysates by means of ultrafiltration with a 100-kDa cutoff filter and titered by using a plaque assay as described previously.[22,23] Intact virus does not go through the filter and is concentrated. Similarly concentrated and purified HeLa cell lysates were used for sham infection.

RV infections

Mice were inoculated with 20 μL of 1×10^8 plaque-forming units (pfu) or sham HeLa cell lysate through the intranasal route under isoflurane anesthesia. Mice were treated on day 6 of life with RV-A1B and day 13 of life with RV-A2

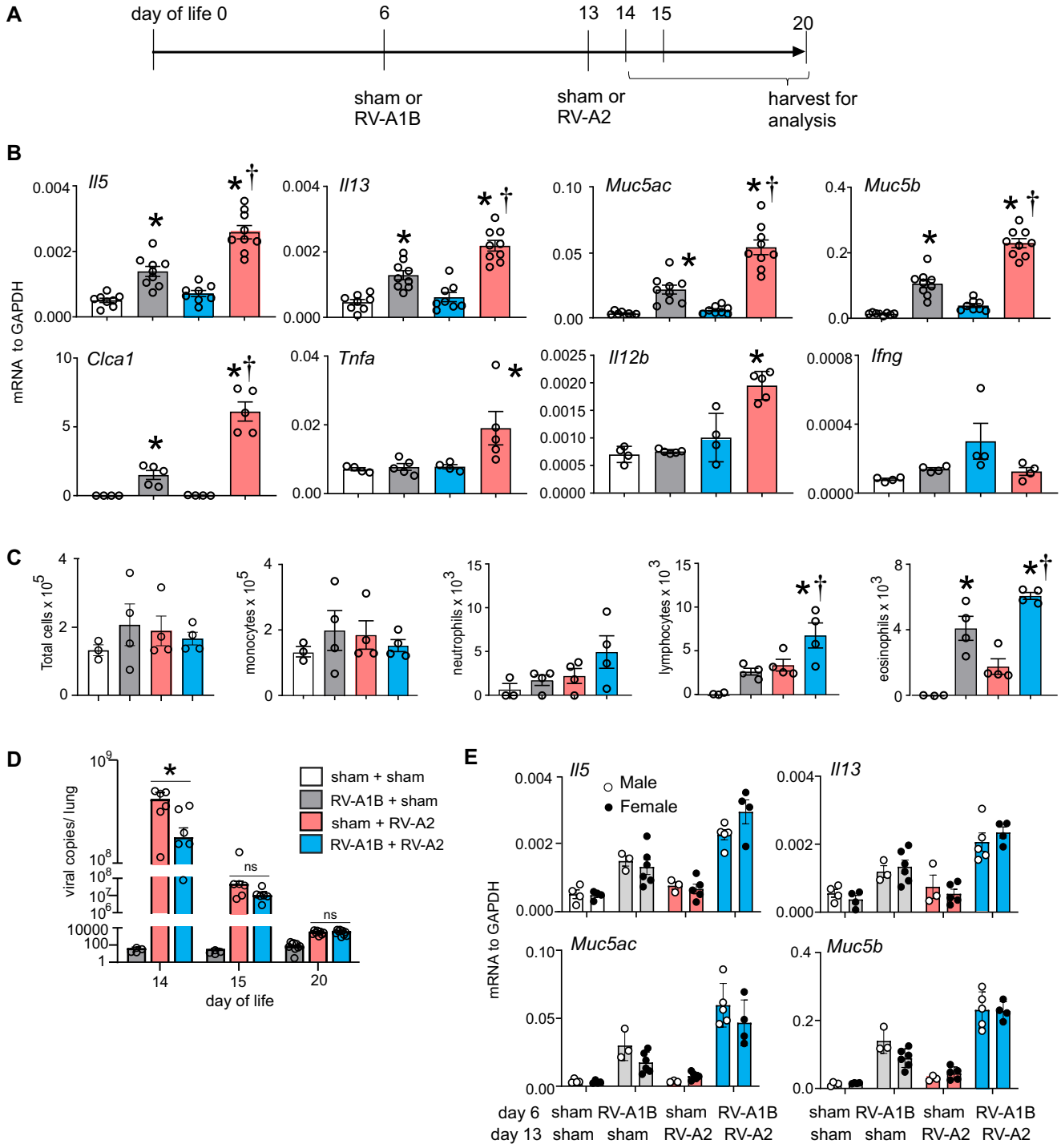

FIG 1. Heterologous RV infection induces exaggerated airway responses. **A**, Baby mice were inoculated with sham or RV-A1B on day 6 of life and with sham or RV-A2 on day 13 of life. **B,** Lungs from sham plus sham–, sham plus RV-A1B–, sham plus RV-A2–, and RV-A1B plus RV-A2–infected mice were harvested on day 20 of life. Shown is lung expression of IL-5, IL-13, IL-5, IFN-γ, Gob5 (Clca1), Muc5b, Muc5ac, TNF-α, and IL-12b mRNA. **C**, BAL inflammatory cell counts for sham plus sham–, sham plus RV-A1B–, sham plus RV-A2–, and RV-A1B plus RV-A2–infected mice. Data shown are means ± SEMs; n = 3 to 9 per group from 2 different experiments; *indicates different from sham plus sham; †indicates different from RV-A1B plus sham; $P < .05$ by 1-way ANOVA and the Tukey multiple comparison test. **D,** RV positive-strand RNA was measured on days 14, 15, or 20 of age (1, 2, or 7 days after RV-A2 infection), and presented as viral copy number in total lung. Data shown are means ± SEMs; n = 4 to 9; *indicates different from day 6 sham plus day 13 RV-A2: $P < .05$, 1-way ANOVA and the Tukey multiple comparison test. **E**, mRNA expression in male and female mice.

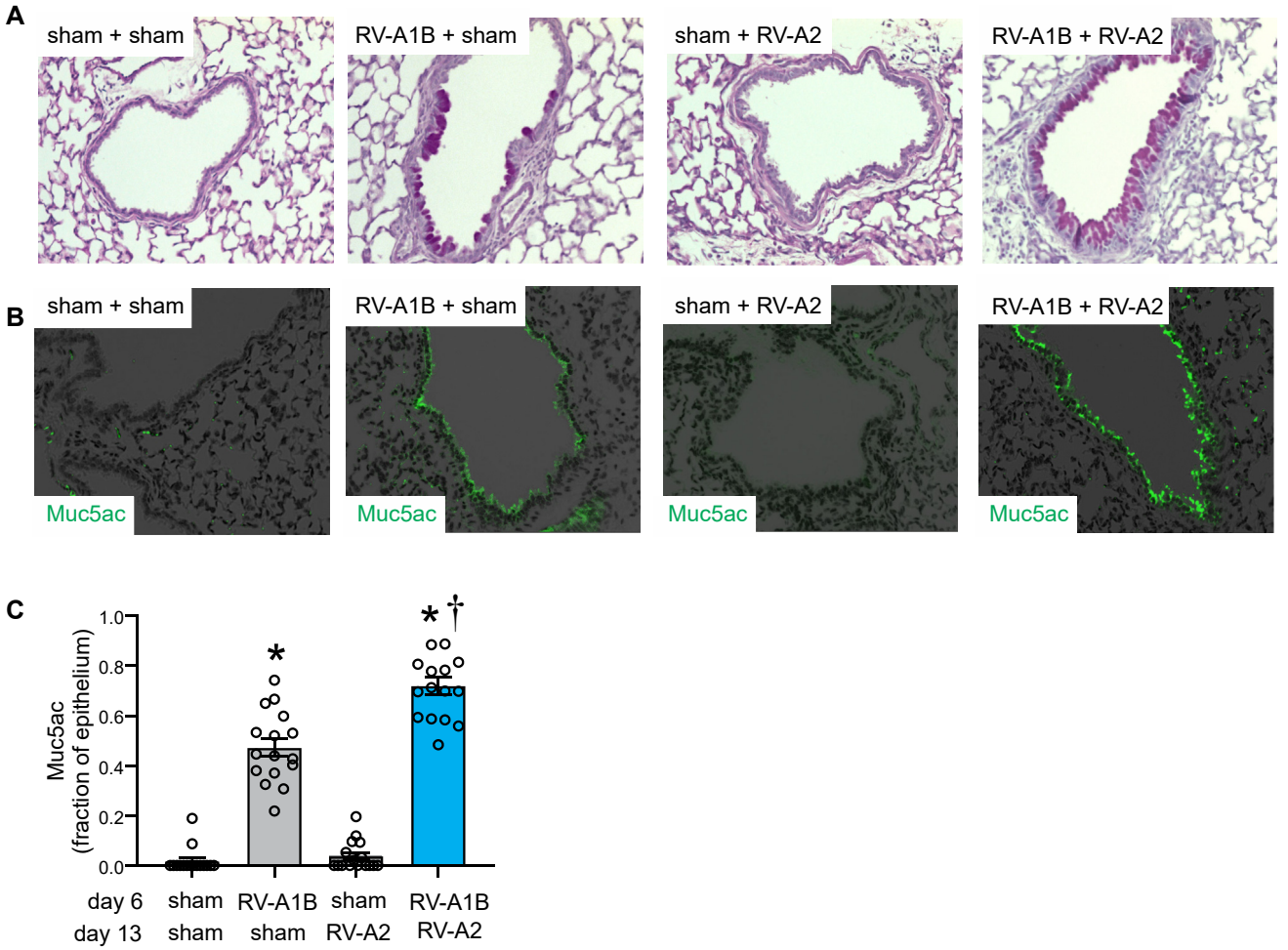

FIG 2. Heterologous RV infection induces exaggerated mucus metaplasia. Baby mice were inoculated with sham or RV-A1B on day 6 and sham or RV-A2 on day 13 of life. Lungs were harvested on day 20 and processed for histology. Lungs sections were stained for PAS and Muc5ac and quantified by using National Institutes of Health ImageJ software. **A**, PAS staining in sham-, RV-A1B–, RV-A2–, and RV-A1B plus RV-A2–infected mice. The black bar is equal to 50 μm. **B**, Muc5ac staining in RV-A1B–, RV-A2–, and RV1B plus RV-A2–infected mice. The white bar is equal to 50 μm. **C**, Quantification of Muc5ac staining in the airways. Data are represented as $Muc5ac^+$ cells per micron of basement membrane length. Images were taken at ×200 magnification. Data shown are means ± SEMs; n = 3 or 4 airways per mouse; 4 mice per group from 2 different experiments; *indicates different from sham plus sham; †indicates different from RV-A1B plus sham; $P < .05$ by 1-way ANOVA and the Tukey multiple comparison test.

as follows: (1) sham on day 6 plus sham on day 13, (2) RV-A1B on day 6 plus sham on day 13, (3) sham on day 6 plus RV-A2 on day 13, and (4) RV-A1B on day 6 plus RV-A2 on day 13 (Fig 1, *A*).

Real-time quantitative PCR

Lungs were harvested at day 20 of life (7 days after the last treatment), and RNA was extracted with Trizol (Invitrogen, Carlsbad, Calif). Lung RNA was isolated by using an RNAeasy kit (Qiagen Germantown, Md). cDNA was synthesized from 2 μg of RNA by using a high-capacity cDNA synthase kit (Applied Biosystems, Foster City, Calif) and subjected to quantitative real-time PCR using specific primers for mRNA (Table E1). The level of gene expression for each sample was normalized to glyceraldehyde-3-phosphate dehydrogenase. Sex was determined by sex-determining region Y (*SRY*) gene expression. To quantify virus particles, quantitative PCR for positive-strand viral RNA (vRNA) was conducted by using RV-specific primers and probes (forward primer, 5′-GTGAAGAGCCSCRTGTGCT-3′; reverse primer, 5′-GCTSCAGGGTTAAGGTTAGCC-3′; and probe, 5′-FAM-TGAGTCCTCCGGCCCCTGAATG-TAMRA-3′).

Lung histology and immunofluorescence

Lungs were harvested at day 20 of life, fixed with 10% formaldehyde overnight, and paraffin-embedded. Blocks were sectioned at 500-μm intervals at a thickness of 5 μm, and each section was deparaffinized, hydrated, and stained. To visualize mucus, sections were stained with periodic acid–Schiff (PAS) (Sigma-Aldrich, St Louis, Mo). Other lung sections were stained with 4′,6-diamidino-2-phenylindole (DAPI) and Alexa Fluor 488–conjugated mouse anti-Muc5ac (clone 45M1 [Thermo Fisher Scientific, Waltham, Mass]) or Alexa-Fluor 488–conjugated anti-CCL11 (Biolegend, San Diego, Calif). IL-13–producing ILC2s and T cells were identified in the airways by immunofluorescence. Lung sections were stained with DAPI, Alexa Fluor 488–conjugated mouse anti-GATA3 (Biolegend), Alexa Fluor 647–conjugated mouse anti-CD3 (Biolegend), and Alexa Fluor 750–conjugated mouse IL-13 (R&D Systems, Minneapolis, Minn). AlexaFluor N-hydroxy succinimidyl esters were purchased from Thermo Fisher. ILC2s were identified as IL-13^+ $GATA3^+$, and T cells were identified as IL-13^+ $GATA3^+$ $CD3^+$.

Images were visualized by using an Axioplan ApoTome microscope with appropriate filters (Carl Zeiss, Thornwood, NY). Muc5ac staining in the

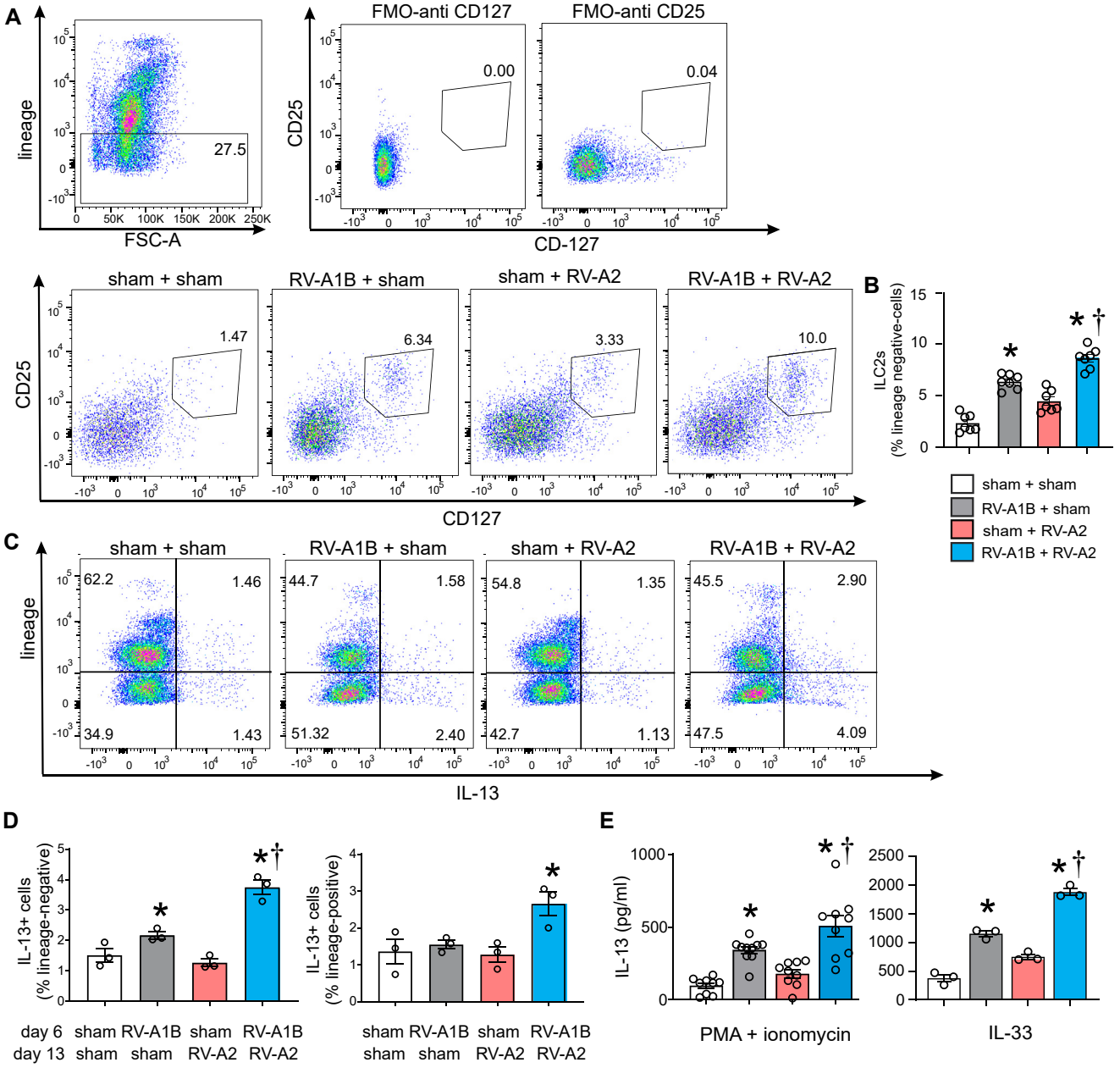

FIG 3. RV infection induces *ILC2* expansion. **A**, Figure showing flow cytometry analysis of live lineage-negative, $CD25^+$ $CD127^+$ ILC2s. **B**, Graph showing group mean data for ILC2s. Data shown are means ± SEMs; n = 7 per group from 3 different experiments; *indicates different from sham plus sham, †indicates different from RV-A1B plus sham; $P < .05$ by 1-way ANOVA and Tukey multiple comparison test. **C,** Flow cytometry analysis of lineage markers and IL-13 in sham, RV-A1B, RV-A2, and RV-A1B plus RV-A2 groups. **D,** Lineage-negative, IL-13^+ cells (*left panel*) and lineage-positive, IL-13^+ cells (*right panel*) for the 4 groups. Data are means ± SEMs; n = 3 per group from 1 experiment; *indicates different from sham plus sham; †indicates different from RV-A1B plus sham; $P < .05$ by 1-way ANOVA and the Tukey multiple comparison test. **E,** IL-13 production from sorted lineage-negative, $CD25^+$ $CD127^+$ ILC2s. ILC2s were stimulated with either phorbol myristate acetate and ionomycin (*left panel*) or IL-33 (*right panel*). Data shown are means ± SEMs; n = 9 or 10 per group from 3 experiments for phorbol myristate acetate and ionomycin stimulation; n = 3 per group from 1 experiment for IL-33 stimulation; *indicates different from sham + sham; †indicates different from RV-A1B + sham; $P < .05$ by 1-way ANOVA and the Tukey multiple comparison test.

airway epithelium, ILC2s, and $CD3^+$ T cells were quantified by National Institutes of Health ImageJ software (Bethesda, Md). Four separate mouse lungs from each of the 4 conditions were processed for sectioning. One section from the mid-left lung was analyzed from each mouse. Between 3 and 5 separate airways of similar size from each lung were chosen for analysis. Muc5ac expression was calculated as the fraction of $Muc5ac^+$ epithelium compared with the total basement membrane length. For cell counts, the average number of cells per airway for each lung is shown.

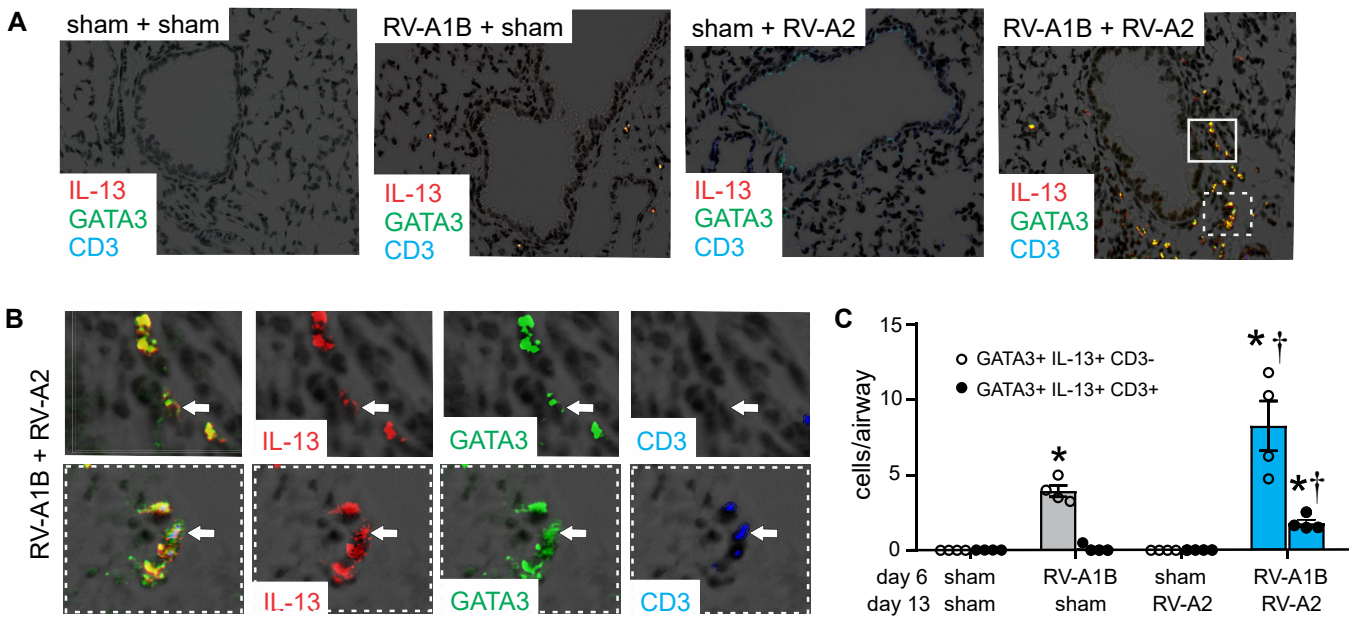

FIG 4. Airway immunofluorescence staining for IL-13, GATA3, and CD3. Baby mice were inoculated with sham or RV-A1B on day 6 of life and sham or RV-A2 on day 13 of life. On day 20, lungs were harvested and fixed with paraformaldehyde. **A,** Lung sections were stained with anti–IL-13 (*red*) anti-GATA3 (*green*), anti-CD3 (*blue*), and DAPI (*black*). Areas of IL-13 and GATA3 colocalization appear in yellow; areas of GATA3 and CD3 colocalization appear in cyan (if IL-13$^-$) or in white (if IL-13$^+$). The white bar is equal to 50 μm. **B**, Color breakdown of areas outlined in panel A. Solid box outlines IL-13$^+$ GATA3$^+$ CD3$^-$ cells; dashed box outlines IL-13$^+$ GATA3$^+$ CD3$^+$ cells. The white bar is equal to 10 μm. **C**, Group mean data showing IL-13$^+$ GATA3$^+$ CD3$^-$ (*open bars*) and CD3$^+$ (*shaded bars*) cells. Each point represents the average of 4 airways from 1 mouse. Data shown are means ± SEMs; *indicates different from sham plus sham; †indicates different from RV-A1B plus sham; $P < .05$ by 1-way ANOVA and the Tukey multiple comparison test.

BAL

Differential counts of bronchoalveolar lavage (BAL) inflammatory cells were performed as described previously.[24]

Flow cytometric analysis

Lungs were perfused with PBS containing EDTA and minced and digested in collagenase IV. Cells were filtered and washed with RBC lysis buffer. For staining with anti–IL-13 antibody, the cells were incubated for 3 hours with cell stimulation cocktail and protein transport inhibitors. Nonspecific binding was blocked by 1% FBS with 1% LPS-free BSA in Dulbecco modified Eagle medium, and 5 μg of rat anti-mouse CD16/32 (Biolegend) was added. To identify ILC2s, cells were stained with FITC-conjugated antibodies for the lineage markers CD3ε, TCRβ, B220/CD45R, Ter-119, Gr-1/Ly-6G/Ly-6C, CD11b (Biolegend), CD11c (Biolegend), TCRβ (Biolegend), F4/80 (Biolegend), FcεRIα (Biolegend), anti-CD25–peridinin-chlorophyll-protein complex (PerCP)-Cy5.5 (eBioscience), and anti-CD127–allophycocyanin (APC; eBioscience), as described.[18] After the staining for cell surface antigens, dead cells were stained with DAPI for flow sorting with live cells or Pac-Blue Live/Dead fixable dead staining dye for further staining with anti–IL-13 antibody (eBioscience). For IL-13 staining, cells were fixed and permeabilized by using permeabilization buffer (eBioscience) and stained with phycoerythrin (PE)-labeled anti–IL-13 antibody (eBioscience). Cells were subjected to flow cytometry on an LSR Fortessa flow cytometer (BD Biosciences, San Jose, Calif), or sorted on a FACSAria II cell sorter (BD Biosciences). Sorted lung ILC2s were cultured *in vitro* and then stimulated with cell stimulation cocktail (phorbol myristate acetate and ionomycin from eBioscience) or recombinant mouse IL-33 (50 ng/mL [Biolegend]). Data were collected by using FACSDiva software (BD Biosciences) and analyzed by using FlowJo software (Tree Star, Ashland, Ore).

Measurement of airway responsiveness

Mice were anesthetized, intubated, and ventilated with a Buxco FinePointe System (Wilmington, NC). Mice were administered increasing doses of nebulized methacholine to assess airway responsiveness, as previously described.[22]

Data analysis

All data were represented as means ± SEs. For studies of airway responsiveness, statistical significance was assessed by 2-way analysis of variance. For all other experiments, statistical significance was assessed by 1-way analysis of variance. Group differences were pinpointed by using the Tukey multiple comparison test.

RESULTS

Heterologous RV infection induces exaggerated airway responses

We found that RV infection of 6-day-old BALB/c mice, but not mature mice, induces an asthma-like phenotype that is associated with ILC2 expansion and dependent on IL-13, IL-25, and IL-33.[18] However, the effects of early-life heterologous infection are unknown. Mice were treated on day 6 of life with RV-A1B and day 13 of life with RV-A2 as follows (Fig 1, *A*): (1) sham on day 6 plus sham on day 13, (2) RV-A1B on day 6 plus sham on day 13, (3) sham on day 6 plus RV-A2 on day 13, and (4) RV-A1B on day 6 plus RV-A2 on day 13. Mice were humanely killed and there lungs harvested at day 20. As seen previously,

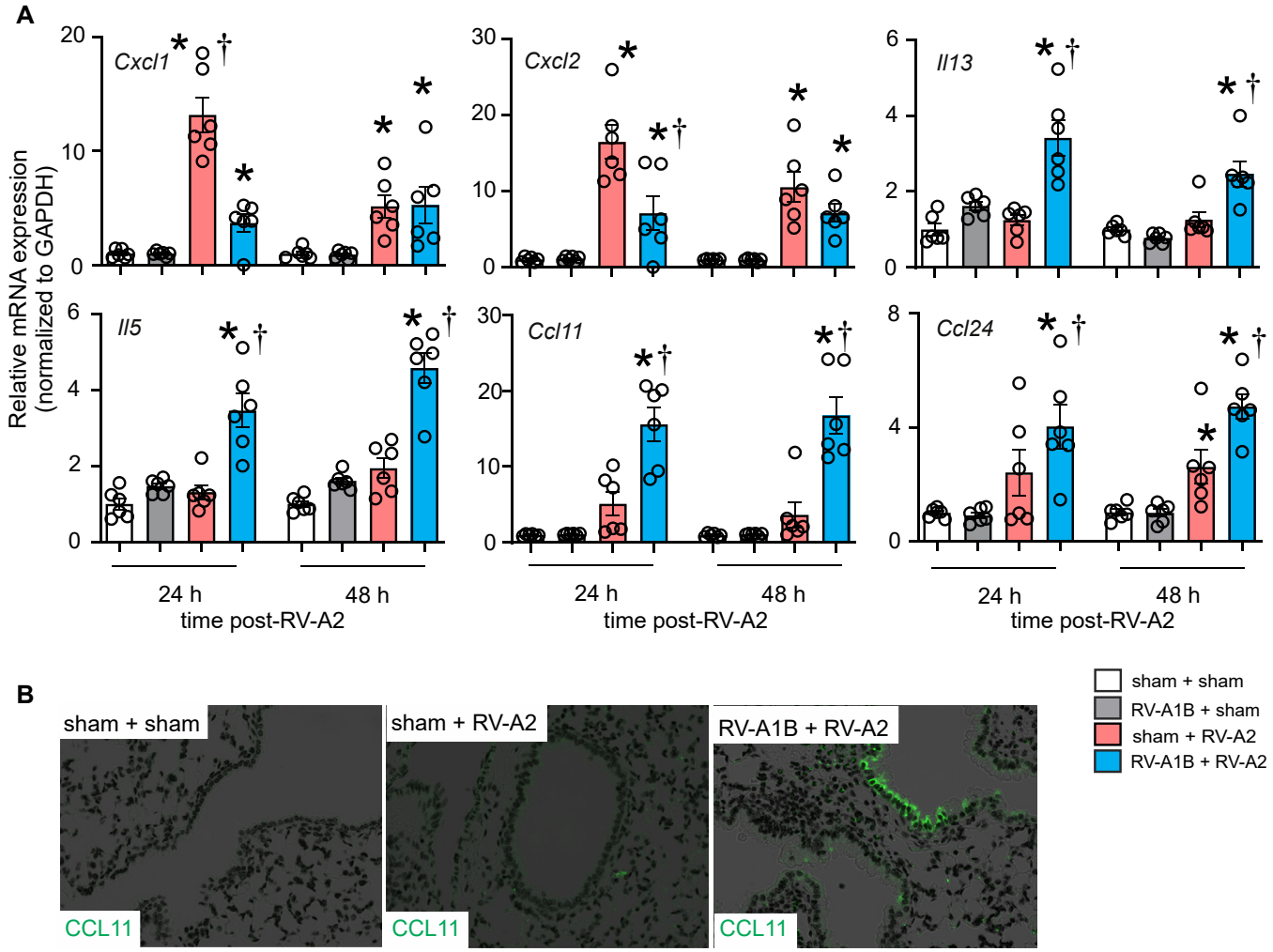

FIG 5. Effect of prior RV-A1B infection on the response to heterologous infection with RV-A2. Baby mice were inoculated with sham or RV-A1B on day 6 of life and sham or RV-A2 on day 13 of life. On days 14 and 15 (ie, 24 and 48 hours after RV-A2 infection), lungs were harvested for mRNA analysis by quantitative PCR or lung immunofluorescence staining. **A**, mRNA expression of CXCL1, CXCL2, IL-13, IL-5, CCL11, and CCL24. Gene expression values were normalized to glyceraldehyde-3-phosphate dehydrogenase (GAPDH) and represented as fold increase over sham plus sham–inoculated mice. Data are means ± SEMs; n = 6 per group from 2 different experiments; *indicates different from sham plus RV-A2; $P < .05$ by 1-way ANOVA and Tukey multiple comparison test. **B**, Lung sections were stained with anti-CCL11 (*shown in green*). White bar = 50 μm.

early-life RV-A1B infection (at day 6 of age) increased total lung expression of the mRNA of the ILC2 products IL-5 and IL-13 and the mucus-related genes *Muc5ac*, *Muc5b*, and *Gob5* (Fig 1, *B*). In contrast, later infection with RV-A2 (on day 13 of life) failed to increase mRNA expression of these genes. IFN-γ mRNA was induced after late RV-A2 infection but not early RV-A1B infection, which is consistent with a mature antiviral response.[18] When we did the reverse experiment and infected 6-day-old mice with RV-A2 and 13-day-old mice with RV-A1B, we got similar results (see Fig E1 in this article's Online Repository at www.jacionline.org).

Next, mice underwent heterologous infection with RV-A1B on day 6 of life and RV-A2 on day 13 of life. These mice demonstrated exaggerated total lung IL-5, IL-13, Muc5ac, Muc5b, and Gob5 mRNA expression that was significantly higher than that induced by RV-A1B alone (Fig 1, *B*). These data suggest that early-life RV-A1B infection shifted the response to subsequent RV-A2 infection from a type 1 to a type 2 response. Consistent with this, expression of IFN-γ mRNA was not increased in mice infected with RV-A1B before day 13 RV-A2 infection. However, total lung expression of TNF and IL-12b mRNA was also exaggerated in mice infected with both RV-A1B and RV-A2. These data show that the effect of heterologous infection does not strictly fit a type 2 model.

Next, we examined BAL inflammatory cell counts in RV-A1B– and RV-A2–treated mice. As shown previously, RV-A1B infection on day 6 of life significantly increased the number of eosinophils in the BAL fluid (Fig 1, *C*). Further, the numbers of eosinophils were significantly increased in mice undergoing heterologous infection compared to mice infected with RV-A1B on day 6 alone. RV-A2 infection on day 13 did not significantly increase eosinophils. There was an increase in lymphocytes in mice undergoing heterologous infection compared to the other groups (Fig 1, *C*).

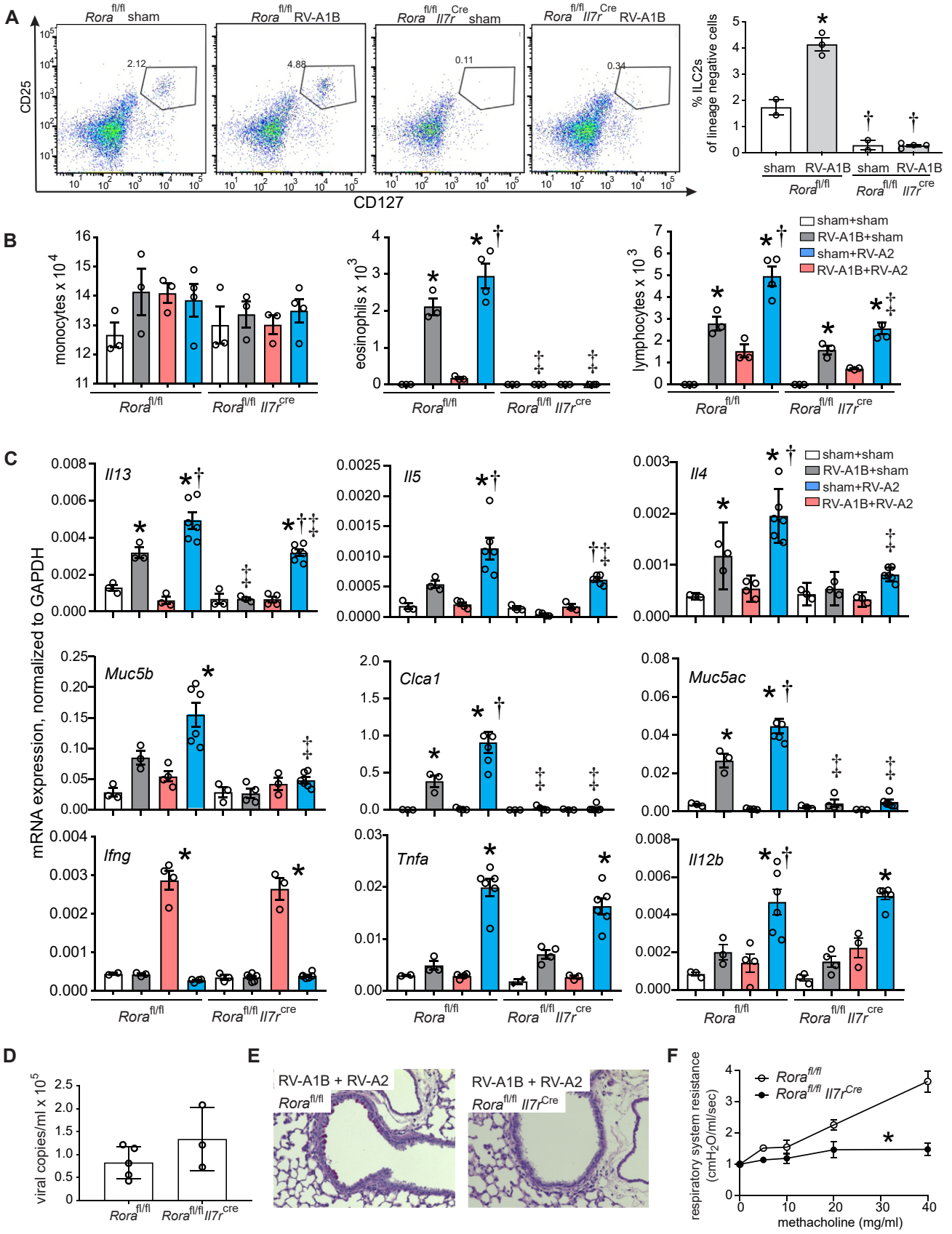
A
Rora fl/fl sham
Rora fl/fl RV-A1B
Rora fl/fl Il7r Cre sham
Rora fl/fl Il7r Cre RV-A1B
CD25
CD127
2.12
4.88
0.11
0.34
% ILC2s of lineage negative cells
sham RV-A1B sham RV-A1B
Rora fl/fl
Rora fl/fl Il7r cre
B
monocytes x 10 4
eosinophils x 10 3
lymphocytes x 10 3
sham+sham
RV-A1B+sham
sham+RV-A2
RV-A1B+RV-A2
C
mRNA expression, normalized to GAPDH
Il13
Il5
Il4
Muc5b
Clca1
Muc5ac
Ifng
Tnfa
Il12b
D
viral copies/ml x 10 5
E
RV-A1B + RV-A2
Rora fl/fl
RV-A1B + RV-A2
Rora fl/fl Il7r Cre
F
respiratory system resistance (cmH2O/ml/sec)
Rora fl/fl
Rora fl/fl Il7r Cre
methacholine (mg/ml)

To determine whether enhanced type 2 inflammatory responses in mice undergoing heterologous infection were due to an increased viral load, we measured lung vRNA levels. First, RV-A1B and RV-A2 infections showed a similar time course of vRNA (see Fig E2, *A* in this article's Online Repository at www.jacionline.org) and infectious virions were detected from mouse lungs infected with either strain (see Fig E2, *B*). When we compared vRNA levels in mice infected with RV-A1B on day 6 and RV-A2 on day 13 with mice infected with RV-A2 on day 13 alone, mice undergoing heterologous infection unexpectedly showed a reduction in viral copies 1 day after RV-A2 infection (Fig 1, *D*), suggesting that early-life RV-A1B infection altered the immune response against subsequent RV-A2 infection. By days 2 and 7 after RV-A2 infection, there were no differences in vRNA level. Finally, there were no significant differences in *Il5*, *Il13*, *Muc5ac*, and *Muc5b* mRNA expression between male and female mice (Fig 1, *E*).

We examined mice for PAS and Muc5ac staining, which is evidence of mucous metaplasia. As shown previously, compared with sham infection, RV-A1B infection on day 6 of life increased PAS staining (Fig 2, *A*). Because PAS detects glycoproteins, carbohydrates, and mucins, staining indicates mucous metaplasia. Infection with RV-A2 on day 13 had no effect on PAS staining. The mice treated with RV1B on day 6 plus RV-A2 on day 13 showed significantly greater PAS staining than did the mice treated with RV1B on day 6 (Fig 2, *A*). Similar results were obtained for deposition of the gel-forming mucin Muc5ac (Fig 2, *B* and *C*), which is further evidence of mucus hypersecretion.

Heterologous infection with RV1B and RV-A2 induces ILC2 expansion and IL-13 production

Next, we examined the effects of heterologous infection on lung ILC2 expansion.

As shown previously,[18] compared with sham infection, RV-A1B infection on day 6 of life increased the number of lung lineage-negative $CD25^+$ $CD127^+$ ILC2s. Compared with infection with RV-A1B alone, heterologous infection with RV-A1B and RV-A2 increased lung ILC2 expansion further (Fig 3, *A* and *B*). Furthermore, when we stained cells for IL-13, most of the IL-13–expressing cells were lineage negative (Fig 3, *C*). Compared with infection with RV-A1B alone, heterologous infection with RV-A1B and RV-A2 increased the number of lung IL-13–expressing lineage-negative cells (Fig 3, *D*). However, heterologous infection also led to an increase in the number lung IL-13–expressing lineage-positive cells when compared with the number in other groups (Fig 3, *D*). When we measured IL-13 production from sorted lung ILC2s, phorbol myristate acetate– and ionomycin-stimulated ILC2s from lungs of mice treated with RV-A1B plus RV-A2 showed increased IL-13 production compared with that in cells from mice infected with RV-A1B alone (Fig 3, *E*). Similar results were obtained when cells were stimulated with IL-33, which is a physiologic agonist.

Finally, we assessed lung ILC2s by immunofluorescence microscopy. Mice infected with RV-A1B on day 6 of life demonstrated significantly increased lung $IL\text{-}13^+$ $GATA3^+$ $CD3^-$ cells, which is consistent with lung ILC2 expansion (Fig 4, *A-C*). Heterologous infection with RV-A2 on day 13 of life further augmented lung ILC2s. Heterologous infection also increased the number of $IL\text{-}13^+$, $GATA3^+$, and $CD3^+$ cells, suggesting IL-13 expression by T_H2 cells.

As already noted, compared with sham-treated mice, mice infected with RV-A1B 7 days before RV-A2 infection on day 13 of life failed to show a mature antiviral response, as was evidenced by the absence of IFN-γ mRNA expression. These data suggest that early-life RV-A1B infection shifted the response to subsequent RV-A2 infection from a type 1 to a type 2 response. To better characterize the effect of early-life RV-A1B infection on the immune response to subsequent heterologous RV infection, we compared airway responses of the sham plus RV-A2 group and the RV-A1B plus RV-A2 group 2 days after RV-A2 infection. Compared with sham infection, preceding RV-A1B infection significantly reduced RV-A2–induced lung expression of CXCL1 and CXCL2 mRNA (Fig 5, *A*). In contrast, prior RV-A1B infection increased mRNA expression of lung CCL11 and CCL24. Immunofluorescence imaging showed increased epithelial cell CCL11 protein expression (Fig 5, *B*).

Rorα$^{fl/fl}$*Il7r*^{cre} mice lacking functional ILC2s demonstrate suppressed type 2 inflammation, eosinophilic inflammation, mucous metaplasia, and airway responsiveness on heterologous infection

The *Rorα*$^{fl/fl}$*Il7r*^{cre} mice lack functional ILC2s.[25] We infected the *Rorα*$^{fl/fl}$*Il7r*^{cre} and *Rorα*$^{fl/fl}$ mice with RV-A1B and determined the number of ILC2s by flow cytometry. *Rorα*$^{fl/fl}$ mice showed expansion of the number of lung ILC2s in response to RV-A1B treatment. *Rorα*$^{fl/fl}$*IL7R*^{cre} showed almost a complete lack of ILC2s (Fig 6, *A*). Next, we determined BAL inflammatory cell

FIG 6. *Rora*$^{fl/fl}$*Il7r*^{cre} ILC2-deficient mice are protected from heterologous infection–induced exaggerated type 2 inflammation and mucous metaplasia. **A,** Flow cytometry analysis of lineage-negative, $CD25^+$ $CD127^+$ ILC2s (n = 2-4 per group). BAL inflammatory cell counts (**B**) and mRNA expression (**C**) in sham plus sham–, RV-A1B plus sham–, sham plus RV-A2–, and RV-A1B plus RV-A2–infected *Rora*$^{fl/fl}$ and *Rora*$^{fl/fl}$*Il7r*^{cre} ILC2-deficient mice. For (**B**) and (**C**), there were 3 to 6 mice per group. For (**A**) to (**C**), data are means ± SEMs; *indicates different from the sham plus sham group of the like mouse strain; †indicates different from RV-A1B plus sham of the like mouse strain; ‡indicates different from the corresponding group in *Rora*$^{fl/fl}$ mouse strain; $P < .05$ by 1-way ANOVA and the Tukey multiple comparison test. **D,** Viral copy number in RV-A1B– plus RV-A2–infected *Rora*$^{fl/fl}$ and *Rora*$^{fl/fl}$*Il7r*^{cre} ILC2-deficient mice. **E,** PAS-stained representative airways from RV-A1B– plus RV-A2–infected *Rora*$^{fl/fl}$ mice (*left*) and *Rora*$^{fl/fl}$*Il7r*^{cre} ILC2-deficient mice (*right*). The black bar is equal to 50 μm. **F,** Changes in total respiratory system resistance in response to inhaled methacholine in anesthetized, tracheotomized *Rora*$^{fl/fl}$ and *Rora*$^{fl/fl}$*Il7r*^{cre} mice. Resistance data were normalized to baseline airway resistance. Data are means ± SEMs for 3 to 10 mice per group measured in 3 different experiments; *indicates different from *Rora*$^{fl/fl}$ mice; $P < .05$ by 2-way ANOVA and the Tukey multiple comparison test.

counts after RV-A1B and RV-A2 treatment. The numbers of eosinophils were significantly increased in RV-A1B–infected $Ror\alpha^{fl/fl}$ mice and further increased in $Rora^{fl/fl}$ mice infected with RV-A1B on day 6 and with RV-A2 on day 13 (Fig 6, *B*). In contrast, $Rora^{fl/fl}Il7r^{cre}$ mice showed almost a complete absence of eosinophils and mucus gene expression. On heterologous infection, $Rora^{fl/fl}Il7r^{cre}$ mice also showed significant but incomplete suppression of IL-5, IL-13, and IL-4 compared to $Rora^{fl/fl}$ mice (Fig 6, *C*). $Rora^{fl/fl}Il7r^{cre}$ mice showed no decrement in TNF-α or IL-12 mRNA expression, demonstrating that ILC2s are not responsible for these cytokines. $Ror\alpha^{fl/fl}Il7r^{cre}$ mice appeared to show a slight increase in viral copy number 7 days after infection (Fig 6, *D*). Finally, compared with similarly treated $Rora^{fl/fl}$ mice, $Rora^{fl/fl}Il7r^{cre}$ mice infected with RV1B on day 6 plus RV-A2 on day 13 showed an absence of PAS staining (Fig 6, *E*) or airway responsiveness (Fig 6, *F*).

DISCUSSION

Early-life wheezing-associated respiratory tract infection by RV is considered a risk factor for asthma development.[1-5] Children are infected with many different RV strains, with infants having 6 to 10 distinct RV infections per year.[8] RV infections do not induce specific immunity to reinfection by heterologous serotypes, even if viruses are from the same species (eg, RV-A1A and RV-A2).[9,10] Recurrent RV infections could result in greater degrees of airway inflammation and the potential for airway remodeling and loss of lung function over time. To test this, we infected wild-type BALB/c mice with RV-A1B on day 6 of life and RV-A2 on day 13 of life. RV infection of 6-day-old mice, but not mature mice, induces an asthma-like phenotype that is associated with ILC2 expansion and dependent on IL-13, IL-25, and IL-33.[18] We found that compared with mice undergoing RV-A1B infection alone, mice undergoing heterologous infection with RV-A1B and RV-A2 showed additive increases in IL-13, IL-5, IL-4, Gob5, Muc5b, and Muc5ac mRNA expression; additive expansion of eosinophils; and exaggerated mucus metaplasia. These data demonstrate that successive RV infections can result in greater degrees of inflammation and mucus production than a single infection does.

These results are more significant when examined in the context of development. By examining the age dependency of RV responses, we previously found that RV induced IL-13 and IL-25 expression in 6-day-old mice, whereas mice aged 8 days and older showed significant IFN-γ expression. Thus, as expected, mice infected with sham on day 6 of life and RV-A2 at day 13 of life showed mature antiviral responses. However, infection with RV-A1B on day 6 life shifted the response to later RV-A2 infection from a type 1 to a type 2 response, as evidenced by increased IL-5 and IL-13 mRNA expression and reduced IFN-γ expression. In addition, compared with sham-infected mice, mice infected with RV-A1B on day 6 and RV-A2 on day 13 of life showed increased lung CCL11 and CCL24 and reduced CXCL1 and CXCL2 mRNA responses, which is consistent with the notion that early-life RV infection alters the host response to heterologous infection, causing a shift toward type 2 inflammation. However, mRNA expression of TNF and IL-12b was also exaggerated in mice infected with both RV-A1B and RV-A2, suggesting that heterologous infection does not strictly fit a type 2 model.

Successive infections with RV-A1B and RV-A2 increased lung expression of IL-5, IL-13, and IL-4 mRNA. ILC2s produce IL-4, IL-5, and IL-13 and are dependent on RORα and GATA3 for their development.[26-30] Accordingly, mice undergoing heterologous infection also showed significant expansion of $CD25^+$ $CD127^+$ ILC2s. Immunofluorescence imaging also showed expansion of $IL\text{-}13^+$ $GATA3^+$ $CD3^-$ cells around the airways. To test the requirement of ILC2s for eosinophilic inflammation and mucous metaplasia, we infected $Ror\alpha^{fl/fl}Il7r^{cre}$ mice lacking functional ILC2s[25] as well as their $Ror\alpha^{fl/fl}$ littermates. Compared with $Rora^{fl/fl}$ mice, $Rora^{fl/fl}Il7r^{cre}$ mice showed complete suppression of BAL eosinophils, mucous metaplasia, and airway hyperresponsiveness. We conclude that early-life heterologous infection with RV-A1B and RV-A2 induces an exaggerated asthma-like phenotype that is dependent on ILC2s.

ILC2s establish their presence in tissues primarily during early postnatal development,[18,31] and increases in tissue ILC2s following infection are mediated through local expansion.[31] Further, pulse-chase experiments in naive adult mice show persistence of IL-5–producing ILC2s for at least 4 weeks, with a substantially lower rate of decay than in labeled $CD4^+$ T cells.[32] We found that ILC2s from lungs of mice treated with RV-A1B plus RV-A2 showed increased IL-13 production compared with that in cells from mice infected on with RV-A1B alone. It is therefore conceivable that lung ILC2s arising after the initial RV-A1B infection form a stable population of innate immune cells capable of responding to subsequent infections, albeit in a nonspecific manner. This concept of "trained immunity" (ie, heterologous immunity attributable to innate immune memory) has been reviewed elsewhere.[20] Future studies, using a longer gap between infections and fate mapping approaches,[31] could answer this question.

Other cells besides ILC2s may be involved in the altered response to heterologous RV infection. Successive infection with RV-A1B and RV-A2 increased the number of lineage-positive IL-13–secreting $GATA3^+$ $CD3^+$ cells. In ILC2-deficient mice, the adaptive T_H2 cell response to protease antigen was impaired because of the loss of ILC2-derived IL-13, which promoted dendritic cell migration to the draining lymph node[33] and production of the T_H2 cell–attracting chemokine CCL17.[34] ILC2s also express the costimulatory molecule OX40L, which is needed for tissue-restricted T-cell costimulation.[35] It is therefore possible that ILC2s cooperate with adaptive T_H2 cells to drive pathologic airway inflammation in response to heterologous viral infection. M2-polarized macrophages could also produce IL-5 and IL-13 in response to heterologous viral infection. In ovalbumin-treated mice, macrophages may produce IL-17 or IL-13 in response to RV-A1B infection, depending on their activation state.[36] Macrophages may also produce IL-5 and IL-13 in response to IL-25 and IL-33.[37] IL-4 and/or IL-13 production by $CD4^+$ T cells and ILC2s activate M2 macrophages required for lung immunity against hookworms.[38] In sputum from patients with asthma, there is a positive correlation between numbers of ILC2s and numbers of M2-polarized macrophages, and coculture of ILC2s with alveolar macrophages induced expression of M2 macrophage-related genes.[39] Finally, we have also demonstrated that compared with sham infection, prior RV-A1B infection increases RV-A2–induced epithelial cell expression of CCL11, which is consistent with the notion that early-life RV infection directly or indirectly alters the response of epithelial cells to subsequent infection.

We would like to mention 2 limitations to our study. First, replication of human RV is minimal in mice. Species differences restrict replication, requiring a high inoculum. However, infection with RV-A1B increases lung type 1 IFN production and negative-strand vRNA expression,[22] which are markers of viral replication. Although replication is limited, the resulting host-induced innate immune response and immunopathology can still be studied. Indeed, replication-deficient viral vectors are a useful tool for studying the innate immune response to acute viral infection without ongoing cytopathic effects.[40] Second, it is difficult to compare the maturity of immature mice and human infants. Although it may be surprising that 6- and 13-day-old-mice, which are still nursing, demonstrate qualitatively different immune responses to viral infection, we have noted previously that the response to respiratory viral infection shifts from an immature type 2 response (characterized by IL-13 and IL-25) to a mature type 1 response (IFN-γ) around 8 days of age.[18] In a subsequent study,[41] we showed that IFN-γ treatment inhibits RV-induced ILC2 function and expansion, suggesting deficient IFN-γ production in 6 day-old mice permits RV-induced type 2 immune responses. Thus, breast-feeding is just 1 indicator of maturity, and it may not reflect structural or functional maturity of the lungs or the development of pulmonary immune function.[42]

We conclude that early-life heterologous infection with RV-A1B and RV-A2 induces an intensified asthma-like phenotype consisting of airway eosinophilic inflammation and mucous metaplasia. Furthermore, early RV infection shifted the immune response to subsequent infection with a heterologous RV strain toward a type 2 response. This model, which is the first preclinical model to combine 2 early-life respiratory viral infections, may provide insight into the development of childhood asthma.

Key messages

- **Early-life (on day 6), RV infection of immature mice induces eosinophilic inflammation and mucous metaplasia, whereas later infection (on day 13) induces a mature type 1 antiviral response.**
- **Early-life infection with RV-A1B skews the immune response to subsequent heterologous infection with RV-A2, causing an exaggerated asthma phenotype unrelated to increased viral load.**
- **ILC2s are required for exaggerated eosinophilic inflammation and mucous metaplasia due to heterologous RV infections.**

REFERENCES

1. Kotaniemi-Syrjanen A, Vainionpaa R, Reijonen TM, Waris M, Korhonen K, Korppi M. Rhinovirus-induced wheezing in infancy–the first sign of childhood asthma? J Allergy Clin Immunol 2003;111:66-71.
2. Lemanske RF Jr, Jackson DJ, Gangnon RE, Evans MD, Li Z, Shult PA, et al. Rhinovirus illnesses during infancy predict subsequent childhood wheezing. J Allergy Clin Immunol 2005;116:571-7.
3. Jackson DJ, Gangnon RE, Evans MD, Roberg KA, Anderson EL, Pappas TE, et al. Wheezing rhinovirus illnesses in early life predict asthma development in high-risk children. Am J Respir Crit Care Med 2008;178.
4. Rubner FJ, Jackson DJ, Evans MD, Gangnon RE, Tisler CJ, Pappas TE, et al. Early life rhinovirus wheezing, allergic sensitization, and asthma risk at adolescence. J Allergy Clin Immunol 2017;139:501-7.
5. Moraes TJ, Sears MR. Lower respiratory infections in early life are linked to later asthma. Thorax 2018;73:105-6.
6. Stein RT, Sherrill D, Morgan WJ, Holberg CJ, Halonen M, Taussig LM, et al. Respiratory syncytial virus in early life and risk of wheeze and allergy by age 13 years. Lancet 1999;354:541-5.
7. Sigurs N, Gustafsson PM, Bjarnason R, Lundberg F, Schmidt S, Sigurbergsson F, et al. Severe respiratory syncytial virus bronchiolitis in infancy and asthma and allergy at age 13. Am J Respir Crit Care Med 2005;171:137-41.
8. Kusel MM, de Klerk NH, Holt PG, Kebadze T, Johnston SL, Sly PD. Role of respiratory viruses in acute upper and lower respiratory tract illness in the first year of life: a birth cohort study. Pediatr Infect Dis J 2006;25:680-6.
9. Rosenbaum MJ, De Berry P, Sullivan EJ, Pierce WE, Mueller RE, Peckenpaugh RO. Epidemiology of the common cold in military recruits with emphasis on infections by rhinovirus types 1A, 2, and two unclassified rhinoviruses. Am J Epidemiol 1971;93:183-93.
10. Minor TE, Dick EC, Peterson JA, Docherty DE. Failure of naturally acquired rhinovirus infections to produce temporal immunity to heterologous serotypes. Infect Immun 1974;10:1192-3.
11. Durrani SR, Montville DJ, Pratt AS, Sahu S, DeVries MK, Rajamanickam V, et al. Innate immune responses to rhinovirus are reduced by the high-affinity IgE receptor in allergic asthmatic children. J Allergy Clin Immunol 2012;130:489-95.
12. van Meel ER, den Dekker HT, Elbert NJ, Jansen PW, Moll HA, Reiss IK, et al. A population-based prospective cohort study examining the influence of early-life respiratory tract infections on school-age lung function and asthma. Thorax 2018;73:167-73.
13. Jackson DJ, Gangnon RE, Evans MD, Roberg KA, Anderson EL, Pappas TE, et al. Wheezing rhinovirus illnesses in early life predict asthma development in high-risk children. Am J Respir Crit Care Med 2008;178:667-72.
14. Oddy WH, de Klerk NH, Sly PD, Holt PG. The effects of respiratory infections, atopy, and breastfeeding on childhood asthma. Eur Respir J 2002;19:899-905.
15. Kusel MMH, de Klerk NH, Kebadze T, Vohma V, Holt PG, Johnston SL, et al. Early-life respiratory viral infections, atopic sensitization, and risk of subsequent development of persistent asthma. J Allergy Clin Immunol 2007;119:1105-10.
16. Culley FJ, Pollott J, Openshaw PJM. Age at first viral infection determines the pattern of T cell–mediated disease during reinfection in adulthood. J Exp Med 2002;196:1381-6.
17. Dakhama A, Park J-W, Taube C, Joetham A, Balhorn A, Miyahara N, et al. The enhancement or prevention of airway hyperresponsiveness during reinfection with respiratory syncytial virus is critically dependent on the age at first infection and IL-13 production. J Immunol 2005;175:1876-83.
18. Hong JY, Bentley JK, Chung Y, Lei J, Steenrod JM, Chen Q, et al. Neonatal rhinovirus induces mucous metaplasia and airways hyperresponsiveness through IL-25 and type 2 innate lymphoid cells. J Allergy Clin Immunol 2014;134:429-39.
19. Han M, Rajput C, Hong JY, Lei J, Hinde JL, Wu Q, et al. The innate cytokines IL-25, IL-33, and TSLP cooperate in the induction of type 2 innate lymphoid cell expansion and mucous metaplasia in rhinovirus-infected immature mice. J Immunol 2017;199:1308-18.
20. Dowling DJ, Levy O. Ontogeny of early life immunity. Trends Immunol 2014;35:299-310.
21. Tuthill TJ, Papadopoulos NG, Jourdan P, Challinor LJ, Sharp NA, Plumpton C, et al. Mouse respiratory epithelial cells support efficient replication of human rhinovirus. J Gen Virol 2003;84:2829-36.
22. Newcomb DC, Sajjan US, Nagarkar DR, Wang Q, Nanua S, Zhou Y, et al. Human rhinovirus 1B exposure induces phosphatidylinositol 3-kinase-dependent airway inflammation in mice. Am J Respir Crit Care Med 2008;177:1111-21.
23. Martin S, Casasnovas JM, Staunton DE, Springer TA. Efficient neutralization and disruption of rhinovirus by chimeric ICAM-1/immunoglobulin molecules. J Virol 1993;67:3561-8.
24. Tsai WC, Rodriguez ML, Young KS, Deng JC, Thannickal VJ, Tateda K, et al. Azithromycin blocks neutrophil recruitment in pseudomonas endobronchial infection. Am J Respir Crit Care Med 2004;170:1331-9.
25. Oliphant CJ, Hwang YY, Walker JA, Salimi M, Wong SH, Brewer JM, et al. MHCII-mediated dialog between group 2 innate lymphoid cells and CD4(+) T cells potentiates type 2 immunity and promotes parasitic helminth expulsion. Immunity 2014;41:283-95.
26. Halim TF, MacLaren A, Romanish MT, Gold MJ, McNagny KM, Takei F. Retinoic-acid-receptor-related orphan nuclear receptor alpha is required for natural helper cell development and allergic inflammation. Immunity 2012;37:463-74.
27. Klein Wolterink RG, Serafini N, van Nimwegen M, Vosshenrich CA, de Bruijn MJ, Fonseca Pereira D, et al. Essential, dose-dependent role for the transcription factor Gata3 in the development of IL-5+ and IL-13+ type 2 innate lymphoid cells. Proc Natl Acad Sci USA 2013;110:10240-5.
28. KleinJan A, Klein Wolterink RG, Levani Y, de Bruijn MJ, Hoogsteden HC, van Nimwegen M, et al. Enforced expression of Gata3 in T cells and group 2 innate

lymphoid cells increases susceptibility to allergic airway inflammation in mice. J Immunol 2014;192:1385-94.
29. Noval Rivas M, Burton OT, Oettgen HC, Chatila T. IL-4 production by group 2 innate lymphoid cells promotes food allergy by blocking regulatory T-cell function. J Allergy Clin Immunol 2016;138:801-11.e9.
30. Pelly VS, Kannan Y, Coomes SM, Entwistle LJ, Rückerl D, Seddon B, et al. IL-4-producing ILC2s are required for the differentiation of TH2 cells following *Heligmosomoides polygyrus* infection. Mucosal Immunol 2016;9:1407.
31. Schneider C, Lee J, Koga S, Ricardo-Gonzalez RR, Nussbaum JC, Smith LK, et al. Tissue-resident group 2 innate lymphoid cells differentiate by layered ontogeny and in situ perinatal priming. Immunity 2019;50:1425-38.e5.
32. Nussbaum JC, Van Dyken SJ, von Moltke J, Cheng LE, Mohapatra A, Molofsky AB, et al. Type 2 innate lymphoid cells control eosinophil homeostasis. Nature 2013;502:245-8.
33. Halim TY, Steer CA, Mathä L, Gold MJ, Martinez-Gonzalez I, McNagny KM, et al. Group 2 innate lymphoid cells are critical for the initiation of adaptive T helper 2 cell-mediated allergic lung inflammation. Immunity 2014;40:425-35.
34. Halim TY, Hwang YY, Scanlon ST, Zaghouani H, Garbi N, Fallon PG, et al. Group 2 innate lymphoid cells license dendritic cells to potentiate memory TH2 cell responses. Nature Immunol 2015;17:57.
35. Halim TY, Rana BM, Walker JA, Kerscher B, Knolle MD, Jolin HE, et al. Tissue-restricted adaptive type 2 immunity is orchestrated by expression of the costimulatory molecule OX40L on group 2 innate lymphoid cells. Immunity 2018;48:1195-207.e6.
36. Hong JY, Chung Y, Steenrod J, Chen Q, Lei J, Comstock AT, et al. Macrophage activation state determines the response to rhinovirus infection in a mouse model of allergic asthma. Respir Res 2014;15:63.
37. Yang Z, Grinchuk V, Urban JF Jr, Bohl J, Sun R, Notari L, et al. Macrophages as IL-25/IL-33-responsive cells play an important role in the induction of type 2 immunity. PLoS One 2013;8e59441.
38. Bouchery T, Kyle R, Camberis M, Shepherd A, Filbey K, Smith A, et al. ILC2s and T cells cooperate to ensure maintenance of M2 macrophages for lung immunity against hookworms. Nature Commun 2015;6:6970.
39. Kim J, Chang Y, Bae B, Sohn K-H, Cho S-H, Chung DH, et al. Innate immune crosstalk in asthmatic airways: Innate lymphoid cells coordinate polarization of lung macrophages. J Allergy Clin Immunol 2019;143:1769-82.e11.
40. Lee BH, Hwang DM, Palaniyar N, Grinstein S, Philpott DJ, Hu J. Activation of P2X7 receptor by ATP plays an important role in regulating inflammatory responses during acute viral infection. PLoS One 2012;7:e35812.
41. Han M, Hong JY, Jaipalli S, Rajput C, Lei J, Hinde JL, et al. IFN-γ blocks development of an asthma phenotype in rhinovirus-infected baby mice by inhibiting type 2 innate lymphoid cells. Am J Respir Cell Mol Biol 2017;56:242-51.
42. Lewin G, Hurtt ME. Pre- and postnatal lung development: An updated species comparison. Birth Defects Res 2017;109:1519-39.

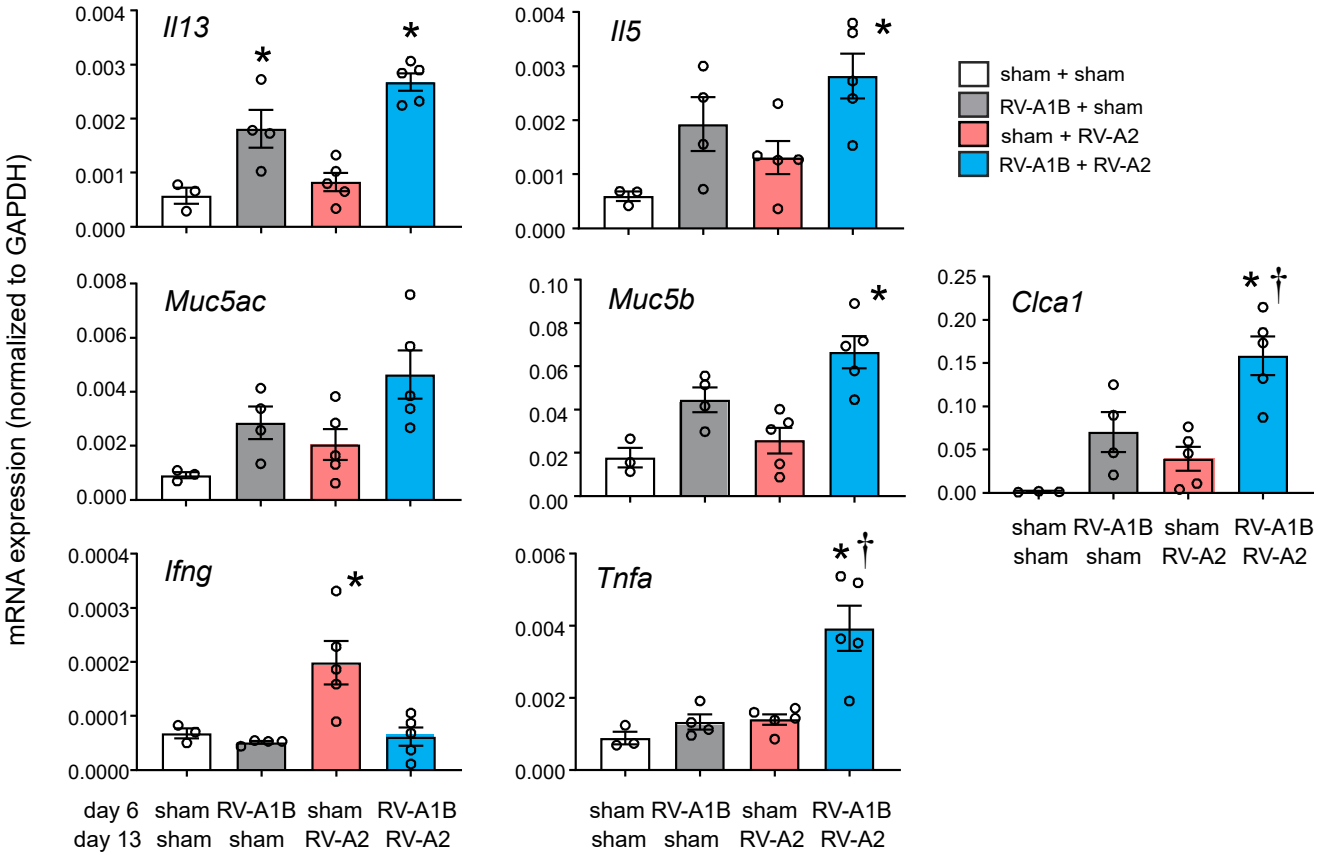

FIG E1. Reversal of RV strain order yields similar airway responses. We infected 6-day-old mice with sham or RV-A2 and 13-day-old mice with sham or RV-A1B. Lungs were harvested on day 20 and processed for RNA analysis. Lung expression of IL-13, IL-5, Muc5ac, Muc5b, Gob5 (*Clca1*), IFN-γ, and TNF-α mRNA was quantified by quantitative PCR. Gene expression values were normalized to glyceraldehyde-3-phosphate dehydrogenase (GAPDH). Data shown are means ± SEMs; n = 3 to 5 per group from 2 different experiments; *indicates different from sham + sham; $P < .05$ by 1-way ANOVA; †indicates different from RV-A1B + sham: $P < .05$ by 1-way ANOVA and the Tukey multiple comparison test.

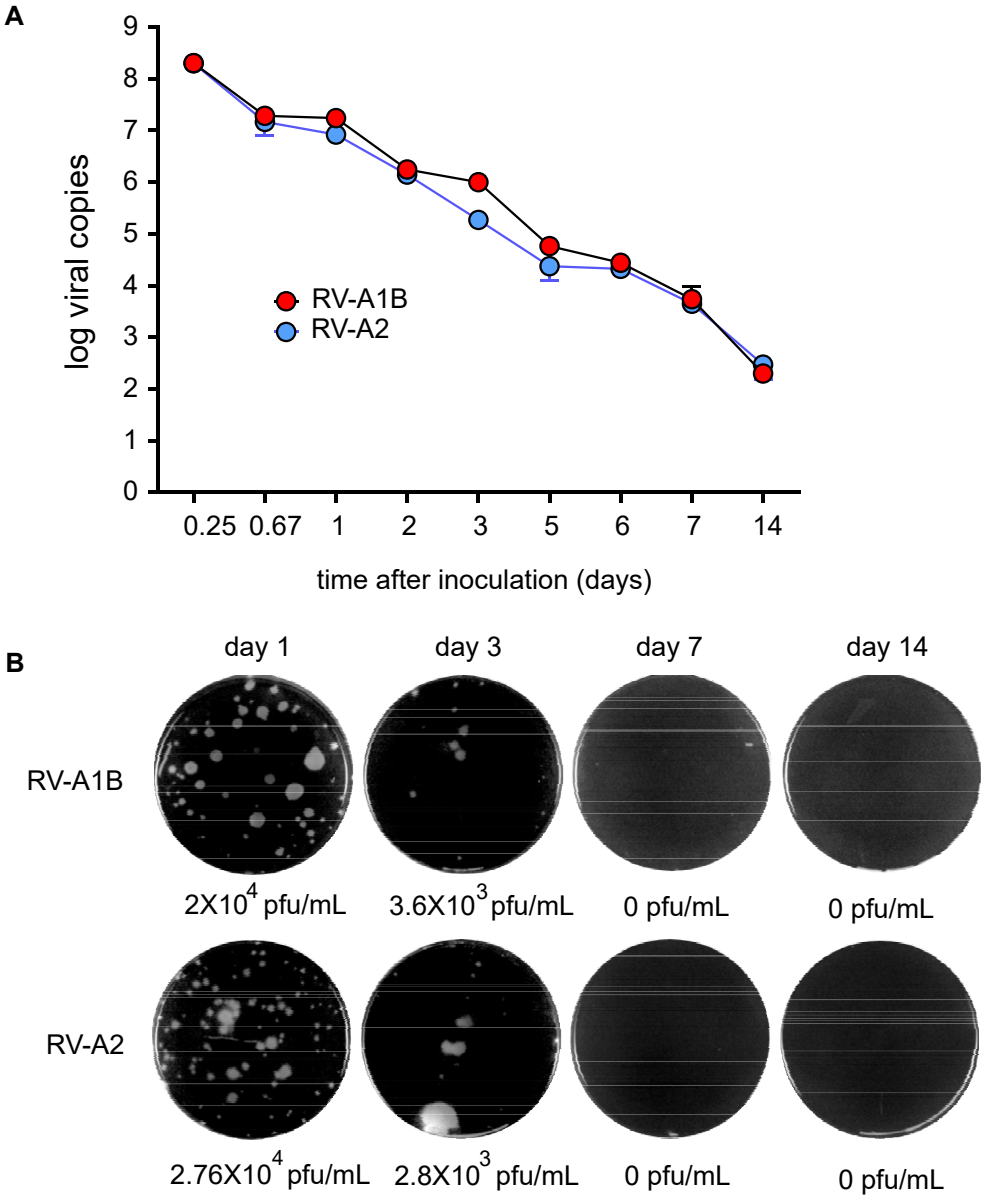

FIG E2. Detection of vRNA and infectious virions from RV-A1B– and RV-A2–infected mice lungs. Six-day-old mice were infected with RV-A1B and RV-2 and harvested at the indicated time points for vRNA analysis (**A**) and plaque assay (**B**). For vRNA, data represent means ± SDs for a sample size of 3 per group from 1 experiment.

TABLE E1. Primer sequences for real-time PCR

Gene	Primer sequences
Gapdh	Forward: 5′-GTCGGTGTGAACGGATTTG-3′
	Reverse: 5′GTCGTTGATGGCAACAATCTC-3′
Clca1	Forward: 5′-CTGTCTTCCTCTTGATCCTCCA-3′
	Reverse: 5′-CGTGGTCTATGGCGATGACG-3′
Ifng	Forward: 5′-ACGCTACACACTGCATCTTGG-3′
	Reverse: 5′-GTCACCATCCTTTTGCCAGTTC-3′
Il12b	Forward: 5′-CTCCTGGTTTGCCATCGTTT-3′
	Reverse: 5′-GGGAGTCCAGTCCACCTCTA-3′
Il13	Forward: 5′-CCTGGCTCTTGCTTGCCTT-3′
	Reverse: 5′-GGTCTTGTGTGATGTTGCTCA-3′
Il5	Forward: 5′-CTCTGTTGACAAGCAATGAGACG-3′
	Reverse: 5′-TCTTCAGTATGTCTAGCCCCTG-3′
Muc5ac	Forward: 5′-AAAGACACCAGTAGTCACTCAGCAA-3
	Reverse: 5′-CTGGGAAGTCAGTGTCAAACC-3′
Muc5b	Forward: 5′-GAGCAGTGGCTATGTGAAAATCAG-3′
	Reverse: 5′-CAGGGCGCTGTCTTCTTCAT-3′
TNFa	Forward: 5′-GCAGGTTCTGTCCCTTTCAC-3′
	Reverse: 5′-GTCGCGGATCATGCTTTCTG-3′
Il4	Forward: 5′-GGTCTCAACCCCCAGCTAGT-3′
	Reverse: 5′-GCCGATGATCTCTCTCAAGTGAT-3′
SRY	Forward: 5′-CGTGGTGAGAGGCACAAGTT-3′
	Reverse: 5′-CTTTAGCCCTCCGATGAGGC-3′

GAPDH, Glyceraldehyde-3-phosphate dehydrogenase.